

Retrieval-enhanced Graph Neural Networks for Graph Property Prediction

Dingmin Wang,¹ Shengchao Liu,^{2*} Hanchen Wang,^{3*} Bernardo Cuenca Grau,¹
Linfeng Song,⁴ Jian Tang,² Song Le,⁵ Qi Li^{6†}

¹ University of Oxford, UK

² Mila - HEC Montréal, Canada, ³ University of Cambridge, UK, ⁴ Tencent, United States

⁵ BioMap and MBZUAI, ⁶ The University of Hong Kong, UK

Abstract

Graph Neural Networks (GNNs) are effective tools for graph representation learning. Most GNNs rely on a recursive neighborhood aggregation scheme, named message passing, thereby their theoretical expressive power is limited to the first order Weisfeiler-Lehman test (1-WL). Motivated by the success of retrieval-based models and off-the-shelf high-performance retrieval systems, we propose a non-parametric and model-agnostic scheme called GRAPHRETRIEVAL to boost existing GNN models. In GRAPHRETRIEVAL, similar training graphs associated with their ground-truth labels are retrieved as an enhancement to be jointly utilized with the input graph representation to complete various graph property predictive tasks. In particular, to effectively “absorb” useful information from retrieved graphs and “ignore” possible noise introduced by potentially irrelevant graphs, we introduce an adapter based on self-attention to explicitly learn the interaction between an input graph and its retrieved similar graphs. By experimenting with three classic GNN models on 12 different datasets, we have demonstrated GRAPHRETRIEVAL is able to bring substantial improvements to existing GNN models without comprising the model size and the prediction efficiency. Our work also firstly validates the feasibility and effectiveness of retrieved-enhanced graph neural networks.

1 Introduction

Graph neural networks (GNNs) are a class of neural architectures for supervised learning which have been adopted in a wide range of applications involving graph-structured data, such as molecule classification (Gilmer et al. 2017a; Liu et al. 2018), recommendation systems (Ying et al. 2018), and knowledge graph completion (Schlichtkrull et al. 2017).

To improve the GNN-based model performance on some downstream tasks, current studies mainly focus on the architecture redesign, and a growing plethora of new GNN models (Kipf and Welling 2017; Gilmer et al. 2017b; Xu et al. 2018; Corso et al. 2020) have been proposed in past few years. Despite newly-designed GNN models have brought improvement in different graph-based predictive tasks, GNN models are still known to suffer some important limitations. These include issues such as limited theoretical expressiveness power due to node-based message passing mechanisms (Balcilar et al. 2021), and example forgetting (Toneva et al. 2019).

*Second and third authors make equal contribution to this paper.

†Corresponding author.

In this paper, we aim at alleviating the example forgetting issue. Motivated by the success of retrieval-based models for NLP (Lewis et al. 2020; Guu et al. 2020; Liu, Yogatama, and Blunsom 2022), we show that the performance of GNN-based models can be significantly enhanced if the training data is also exploited at testing time for making predictions. This is in contrast to the standard setting in supervised learning, where the training data is typically discarded once training has been completed and the model relies solely on the learned parameters for making predictions.

We focus on graph classification and regression tasks using GNNs. Given training examples consisting of graph-label pairs (\mathcal{G}_i, l_i) , where nodes in the graphs are annotated with numeric feature vectors, our aim is to learn a model that predicts label l given an input graph \mathcal{G} . At training time, GRAPHRETRIEVAL consists of the following steps.

1. *Standard supervised training.* Initially, we train the GNN-based model of interest from examples in the usual way, and obtain a trained model \mathcal{M} as a result.
2. *Indexing.* We apply \mathcal{M} to each of the training examples $\{(\mathcal{G}_1, l_1), \dots, (\mathcal{G}_n, l_n)\}$ and obtain the corresponding graph-level representation vectors $h_{\mathcal{G}_1}, \dots, h_{\mathcal{G}_n}$. We then construct a key-value index having vectors $h_{\mathcal{G}_i}$ as the key and the corresponding example (\mathcal{G}_i, l_i) as value.
3. *Self-attention based adapter.* The adapter is parameterized with two learnable matrices \mathbf{W}_1 and \mathbf{W}_2 which can be optimised using the training data after the model \mathcal{M} and the index have been obtained.

Given an input graph \mathcal{G} at testing time, we compute its label l according to the following steps.

1. *Standard GNN application.* We apply \mathcal{M} to \mathcal{G} to obtain its representation vector $h_{\mathcal{G}}$ and its corresponding initial label $l_{\mathcal{G}}$ in the usual way.
2. *Graph retrieval.* We rank the representation vectors in the index according to their L2 similarity to $h_{\mathcal{G}}$, and retrieve the top- k vectors $\{h_{\mathcal{G}_{i_1}}, \dots, h_{\mathcal{G}_{i_k}}\}$ with highest similarity score; we then retrieve the corresponding example graphs and labels $(\mathcal{G}_{i_1}, l_{i_1}), \dots, (\mathcal{G}_{i_k}, l_{i_k})$.
3. *Self-attention.* Based on the learned adapter and \mathcal{M} , we compute the final output label l as a weighted sum of the initially predicted label $l_{\mathcal{G}}$ and the labels l_{i_1}, \dots, l_{i_k} of the retrieved training examples.

We have implemented our approach and used it to enhance three strong GNN baselines, GCN (Kipf and Welling 2017), GIN (Xu et al. 2018), and PNA (Corso et al. 2020). The effectiveness and feasibility of GRAPHRETRIEVAL are evaluated on 12 benchmarks, including two image datasets, eight molecule datasets, and two large-scale quantum chemistry datasets. Our main contributions are summarized as follows:

- Three GNN models equipped with GRAPHRETRIEVAL achieve substantial improvements on all twelve datasets.
- The adapter contains very few parameters and the high-performance retrieval system (FAISS (Johnson, Douze, and Jegou 2019) introduces negligible time cost, so GRAPHRETRIEVAL is general argumentation component to existing GNN models without compromising the model complexity and the prediction efficiency.
- We perform extensive ablations to study the design choices of our model to justify their effectiveness.

2 Background

In this section, we recapitulate the basics of GNNs and formulate the relevant graph classification and regression tasks.

Message-passing GNNs

In the context of GNNs, we define a graph \mathcal{G} as a tuple

$$(\mathcal{V}, \mathcal{E}, \{\mathbf{x}_v\}_{v \in \mathcal{V}}, \{\mathbf{x}_e\}_{e \in \mathcal{E}}),$$

where \mathcal{V} is a set of nodes with each node $v \in \mathcal{V}$ annotated with a numeric feature vector \mathbf{x}_v , and \mathcal{E} is a set of (undirected) edges where each edge $e \in \mathcal{E}$ is also annotated with a feature vector \mathbf{x}_e . For instance, in a molecule classification scenario, nodes may represent molecules, edges represents bonds between molecules, and feature vectors encode information about atoms and bond types.

When given a graph $\mathcal{G} = (\mathcal{V}, \mathcal{E}, \{\mathbf{x}_v\}_{v \in \mathcal{V}}, \{\mathbf{x}_e\}_{e \in \mathcal{E}})$ as input, a message-passing GNN (Gilmer et al. 2017b) with T layers updates each node feature vector throughout by aggregating messages from its neighbors. Formally, for each layer $1 \leq t \leq T$ and each node $v \in \mathcal{V}$, the feature vector $\mathbf{h}_v^{(t)}$ for node v in layer t is computed as follows:

$$\mathbf{m}_v^{(t)} = \sum_{\{u, v\} \in \mathcal{E}} M_{t-1}(\mathbf{h}_v^{(t-1)}, \mathbf{h}_u^{(t-1)}, x_{\{u, v\}}), \quad (1)$$

$$\mathbf{h}_v^{(t)} = U_t(\mathbf{h}_v^{(t-1)}, \mathbf{m}_v^{(t)}), \quad (2)$$

where $\mathbf{h}_v^{(0)} = \mathbf{x}_v$ for each $v \in \mathcal{V}$, and where M_t and U_t represent the GNN’s message passing and update functions in the t -th layer, respectively. The concrete description of these functions is given in terms of the learnable parameters of the model. Finally, a ReadOut function is applied on the node feature vectors in the outermost layer $t = T$ to obtain a graph-level representation vector:

$$\mathbf{h}_{\mathcal{G}} = \text{AGG}\left(\left\{\mathbf{h}_v^{(T)} \mid v \in \mathcal{G}\right\}\right), \quad (3)$$

where **AGG** can be any permutation-invariant operation on multi-sets applied to a vector in a component-wise manner, such average, summation or attention-based aggregation.

Graph Classification and Regression

Given the graph-level representation vector $\mathbf{h}_{\mathcal{G}}$ for an input graph \mathcal{G} , there are usually two prediction tasks of interest:

1. *classification*, where a multi-layer perceptron (MLP) followed by the application of a non-linear activation function is used to map $\mathbf{h}_{\mathcal{G}}$ to one of predefined classes; and
2. *regression*, where an MLP maps $\mathbf{h}_{\mathcal{G}}$ to a numeric value.

For a binary classification task (e.g., MolHIV classification task) we normally use the sigmoid function and hence the final class label is obtained as follows:

$$l^{\mathcal{G}} = \text{Sigmoid}(\text{MLP}(\mathbf{h}_{\mathcal{G}})). \quad (4)$$

In multi-class *classification* tasks (e.g, MNIST recognition task (LeCun et al. 1998)), we usually apply the SoftMax function, and the output class label is obtained as follows:

$$l^{\mathcal{G}} = \text{SoftMax}(\text{MLP}(\mathbf{h}_{\mathcal{G}})). \quad (5)$$

For *regression* tasks (e.g., the PCQM4M regression task (Nakata and Shimazaki 2017)), the output value is obtained directly from the MLP as follows:

$$l^{\mathcal{G}} = \text{MLP}(\mathbf{h}_{\mathcal{G}}). \quad (6)$$

3 Methodology

In this section we describe the technical details of GRAPHRETRIEVAL to graph classification and regression tasks. The different steps are schematically depicted in Figure 1.

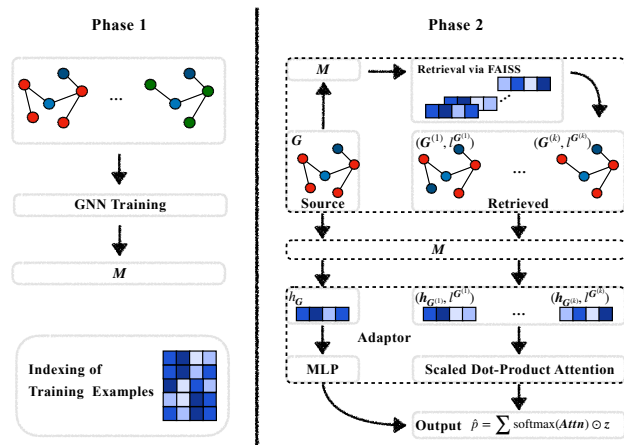


Figure 1: Scheme of GRAPHRETRIEVAL. In the Phase 1, we first train a GNN named \mathcal{M} with a labelled dataset. Then, we index the training graphs into FAISS. In the stage 2, for each input graph we use a pre-trained GNN \mathcal{M} to retrieve most similar graphs from the training data and further train an adaptor module to integrate the retrieved information.

In what follows, we fix an arbitrary set of training examples $\{(\mathcal{G}_1, l_1), \dots, (\mathcal{G}_n, l_n)\}$ consisting of pairs (\mathcal{G}_i, l_i) of a graph \mathcal{G}_i and a corresponding prediction l_i (i.e., a class label in the case of classification, or a number in the case of regression). Furthermore, we fix a GNN given by a set of message-passing, update, and ReadOut functions as described in Section 2.

Phase 1: Initial Training and Indexing

GNN Training The first step in our approach is to train the GNN in a standard supervised way using the given examples. As a result, we obtain a trained GNN model \mathcal{M} with concrete values for each of the parameters of the model; these parameter values will remain fixed in all subsequent steps.

Indexing of Training Examples After training, we apply \mathcal{M} to each of the example graphs $\mathcal{G}_1, \dots, \mathcal{G}_n$ and obtain the corresponding graph-level representation vectors $h_{\mathcal{G}_1}, \dots, h_{\mathcal{G}_n}$ as described in Equation (3). We then input key value pairs $[h_{\mathcal{G}_i}, (\mathcal{G}_i, l_i)]$ for each $1 \leq i \leq n$ to the FAISS retrieval engine (Johnson, Douze, and Jegou 2019) to construct an index from these key-value pairs. Using a FAISS index will significantly facilitate the retrieval of similar graphs at testing time. It is worth emphasizing that the index only needs to be constructed once throughout our entire pipeline.

Phase 2: Training Self-attention Based Adapter

Given an input graph \mathcal{G} , we compute the corresponding prediction l according to the following steps.

First, we apply the trained GNN \mathcal{M} to \mathcal{G} to obtain, in the usual way, an initial prediction $l_{\mathcal{G}}$ and graph-level representation $h_{\mathcal{G}}$. The main novelty in our approach, however, lies in the following two steps, where we first retrieve a set of most similar graphs from the index and subsequently exploit self-attention to compute the final prediction l . We next describe these steps in detail.

Graph Retrieval. In this step, we use the FAISS index to find the top- k vectors $\{h_{\mathcal{G}_{i_1}}, \dots, h_{\mathcal{G}_{i_k}}\}$ that are most similar to $h_{\mathcal{G}}$, and to subsequently retrieve the corresponding example graphs and labels $(\mathcal{G}_{i_1}, l_{i_1}), \dots, (\mathcal{G}_{i_k}, l_{i_k})$. The value k is considered a hyper-parameter in our approach, and we use L2 distance to compute vector similarity scores.¹

Note that, since the index is built from the training dataset, the most similar graph for each input graph is always itself during the training stage. Inspired by (Jiang et al. 2021) and to reduce overfitting, we also adopt the *retrieval dropout* strategy. Specifically, during the training stage, we will retrieve $k + 1$ graphs, in which the most similar graph will be dropped. In the evaluation stage, *retrieval dropout* is disabled, as evaluation graphs are usually not part of the training data.

Sel-attention Based Adapter Inspired by the transformer proposed in (Vaswani et al. 2017), we exploit self-attention to compute the final prediction l for input graph \mathcal{G} as a weighted sum of the initially predicted label $l_{\mathcal{G}}$ and the top- k example labels l_{i_1}, \dots, l_{i_k} with respective weights w_0, \dots, w_k .

The self-attention mapping takes as input a *query vector* and a set of key-value pairs and yields the weights w_0, \dots, w_k . In our setting, the query vector \mathbf{q} is obtained by multiplying a learnable matrix \mathbf{W}_1 to the graph-level representation $h_{\mathcal{G}}$ for the input \mathcal{G} :

$$\mathbf{q} = \mathbf{W}_1 h_{\mathcal{G}}, \quad (7)$$

¹Recall that, given d -dimensional vectors v^1 and v^2 , the L2 distance between v^1 and v^2 is given by $\sqrt{\sum_{i=1}^d (v_i^1 - v_i^2)^2}$

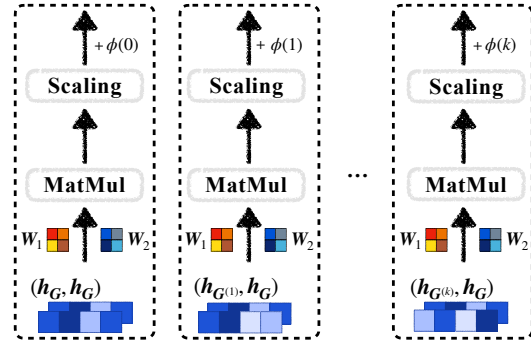


Figure 2: Scheme on Scaled Dot Product Attention.

In turn, to obtain the keys, we pack the $k + 1$ graph representations $\{h_{\mathcal{G}}, h_{\mathcal{G}_{(i_1)}}, \dots, h_{\mathcal{G}_{(i_k)}}\}$ as row vectors into a matrix \mathbf{H} , and then multiply \mathbf{H} with a learnable matrix \mathbf{W}_2 to obtain matrix

$$\mathbf{K} = \mathbf{W}_2 \mathbf{H}, \quad (8)$$

Finally, the attention weights $\mathbf{Attn} = (w_0, \dots, w_k)$ are obtained by computing the scaled product of \mathbf{q} with the transpose of \mathbf{K} and adding a $(k + 1)$ learnable bias vector \mathbf{b}

$$\mathbf{Attn} = \frac{\mathbf{q} \mathbf{K}^T}{\sqrt{d}} + \mathbf{b}, \quad (9)$$

where d is the dimension of the query vector \mathbf{q} . Intuitively, the bias vector \mathbf{b} allows the model to encode the ranking between the different retrieved graphs; without it, the model cannot distinguish between the different retrieved graphs and the ranking information is lost as a result.

Computing the final prediction. Once the attention weights have been obtained, we can compute the output prediction as a weighted sum. Specifically, we compile the initially predicted label $l_{\mathcal{G}}$ and the top- k example labels l_{i_1}, \dots, l_{i_k} into a vector \mathbf{z} and obtain the final output as:

$$l = \sum \text{softmax}(\mathbf{Attn}) \odot \mathbf{z}, \quad (10)$$

where \odot is the element-wise (Hadamard) product.

Two-phase Model Training

The overall training pipeline is illustrated in Algorithm 1. We use cross entropy and mean square error as the loss functions for classification and regression tasks, respectively.

Lines 1–4 correspond to the initial training of the GNN model and the construction of the index. In Lines 5–7 we train the adapter module and optimise the values in the learnable matrices \mathbf{W}_1 and \mathbf{W}_2 and the bias vector \mathbf{b} described in Section 3, where the GNN model \mathcal{M} is fixed.

Finally, when learning \mathbf{W}_1 and \mathbf{W}_2 from the training data using our entire pipeline, it is worth noticing that the most similar graph of an example graph \mathcal{G}_i will be itself, so we will always drop it and consider only the other retrieved graphs.

Algorithm 1: Pipeline of Two-phase Model Training

Require: Training and validation datasets; randomly initialised GNN and Adapter; training epochs m_1 for GNN and m_2 for the adapter; number of retrieved graphs k .

- 1: **for** $i = 1$ **to** m_1 **do**
- 2: Train the GNN model over the training dataset. Optimal GNN parameters of a trained model \mathcal{M} is saved by evaluating on the validation dataset.
- 3: **end for**
- 4: Construct FAISS index.
- 5: **for** $i = 1$ **to** m_2 **do**
- 6: Train the Adapter over the train set using the index and the fixed model \mathcal{M} . Optimal parameters of Adapter is saved by evaluating on the validation dataset.
- 7: **end for**
- 8: **return** \mathcal{M} and Adapter defined by W_1, W_2, b .

4 Experiments

In this section, we conduct comprehensive experiments on 12 datasets to answer the following three questions:

- **Q1:** Is it good enough to only use the graph retrieval?
- **Q2:** Why do we need to use the self-attention?
- **Q3:** How much gains can GRAPHRETRIEVAL bring to graph neural network based models?

Benchmark Dataset

We used a collection of 12 datasets consisting of 8 small-scale molecule datasets, 2 computer vision datasets, and 2 large-scale quantum chemistry datasets. The molecule datasets and the computer vision datasets focus on classification tasks, while PCQM4M and PCQM4Mv2 datasets are relevant for regression tasks. For MNIST and CIFAR10, we pre-process the images into grids before applying GNNs. For a fair comparison, we follow the standard train/valid/test splits for all datasets according to *ogb*² and *torch-geometric*.³ In particular, for the molecule datasets, we use *scaffold split* (Ramsundar et al. 2019), where molecules are split according to their scaffold (molecular substructure). We used a conventional random split for the remaining datasets.

Baseline Models

We adopt three widely-used GNN baselines: Graph Convolutional Networks (GCN) (Kipf and Welling 2017), Graph Isomorphism Networks (GIN) (Xu et al. 2018), and Principal Neighbourhood Aggregation (PNA) (Corso et al. 2020).

Besides, we adopt two purely retrieval-based approaches, denoted as *Retrieval*, which retrieves the most similar graph from the FAISS index whose label is as our predicted answer; and *Majority-voting*, which retrieves some number of the most similar graphs from the FAISS index whose labels will be ranked based on their frequency, and then we choose the most frequent label as our predicted answer.

²<https://github.com/snap-stanford/ogb>

³https://github.com/pyg-team/pytorch_geometric

Training Details

GRAPHRETRIEVAL is model-agnostic framework and can be applied to enhance a wide range of GNN models. Training is conducted as described in Algorithm 1, where $m_1 = 300$, $m_2 = 200$ and $k = 3$. We use the Adam optimizer (Kingma and Ba 2015) with an initial learning rate 0.01 and decay the learning rate by 0.5 every 50 epochs for all the GNN baselines. Batch normalization (Ioffe and Szegedy 2015) is applied on every hidden layer. Some hyperparameters for the three baseline GNN models are shown in Phase 2 of the training (Lines 5–7) is repeated 5 times with different initialisation seeds for W_1 , W_2 , and b ; we report the mean and standard deviation of the values obtained in these runs.

Experimental Results

Predict with only graph retrieval (Q1). Here, we explore whether only using the retrieved results is good enough to achieve a good prediction. We compare *Retrieval* and *Majority-voting* methods against three well trained models on four datasets: CIFAR10, MNIST, PCQM4M and PCQM4Mv2. In particular, for Majority-voting method, we try three different retrieved numbers (5, 10 and 20) to see their performance on four different datasets.

From Table 2, we can clearly see that both *Retrieval* and *Majority-voting* method greatly underperform the three well-trained models. In the CIFAR10 dataset, *Retrieval* methods have more than 15% accuracy loss when compared with the other three well-trained GNN models. For Majority-voting method, we can notice that as we increase the number of retrieved graphs from 10 to 20, the accuracy decreases on both CIFAR10 and MNIST datasets. One straightforward reason might be that as the number of retrieved results increases, the number of noisy labels will increase accordingly. For PCQM4M and PCQM4Mv2 datasets, we can observe that *Majority-voting* method performs the same regardless of the changes of the number of retrieved results. The reason is that in PCQM4M and PCQM4Mv2 datasets where the label is not a discrete value, we notice that each of retrieved results from PCQM4M and PCQM4Mv2 datasets has a different label and the label frequency is always 1. Since we take the label of the most similar graph as our predicted answer, *Majority-voting* method thus degrades to behave the same as Retrieval-only method. This explains why using different retrieved numbers in *Majority-voting* method, we obtain the same MAE scores on both PCQM4M and PCQM4Mv2 datasets.

Self-attention VS Averaging (Q2). One intuition about using the self-attention is that we hope to assign different weights to different retrieved results according to their relevance with respect to the target graph. Here, to demonstrate the necessity and the effectiveness of using the self-attention mechanism in our framework, we compare a self-attention setting against an averaging setting. Assume we have a predicted label l_G from the trained GNN \mathcal{M} and k labels $\{l_1, \dots, l_k\}$ from the retrieved results, we need to output a predicted answer. The self-attention mechanism refers to the phase 2 described in Section 3, in which we assign different weights to the $k + 1$ labels $\{l_1, \dots, l_k, l_G\}$ and then get the predicted answer based the weighted sum as shown in Equation 10.

Table 1: Test set ROC-AUC (%) performance on 8 molecule datasets.

	BBBP	Tox21	ToxCast	SIDER	ClinTox	MUV	HIV	BACE	Average
GCN	70.0	73.9	64.0	58.6	92.2	75.9	78.6	81.9	74.4
GIN	70.5	74.9	64.5	58.7	87.0	76.8	77.0	74.8	73.0
PNA	70.0	73.0	62.0	58.0	87.0	71.0	77.0	72.0	71.2
GRAPHRETRIEVAL-GCN	71.0	75.9	65.4	60.8	93.2	77.7	80.8	84.1	76.1 (1.7%↑)
GRAPHRETRIEVAL-GIN	71.9	77.3	67.4	61.5	89.2	78.4	79.5	81.2	75.8 (2.8%↑)
GRAPHRETRIEVAL-PNA	71.5	75.4	63.1	59.8	89.0	72.9	78.0	79.9	73.7 (2.5%↑)

Table 2: Experimental results of different methods on the four different testing datasets. The evaluation metric for CIFAR10 and MNIST is accuracy and MAE for PCQM4M and PCQM4Mv2. Number in the bracket of *Majority-voting* method represents the retrieved number.

	CIFAR10	MNIST	PCQM4M	PCQM4Mv2
GCN	0.647	0.960	0.171	0.139
GIN	0.656	0.968	0.157	0.123
PNA	0.687	0.972	–	–
Retrieval	0.491	0.853	1.983	1.861
Majority-voting (5)	0.517	0.871	1.983	1.861
Majority-voting (10)	0.519	0.889	1.983	1.861
Majority-voting (20)	0.487	0.842	1.983	1.861

For the averaging setting, we take the average value of $k + 1$ labels as our predicted without distinguishing their degree of importance to our prediction.

Table 3: Experimental results of Self-attention VS Averaging on four datasets. The base model we use is GCN.

-	CIFAR10	MNIST	PCQM4M	PCQM4Mv2
Self-attention	0.676	0.972	0.160	0.120
Averaging	0.577	0.921	0.313	0.214

From Table 3, we can observe that incorporating the self-attention mechanism into our framework significantly outperforms than using the averaging scheme. In CIFAR10 dataset, using the self-attention mechanism achieves an about 10% accuracy improvement over the averaging scheme. One possible reason is that constrained by the performance of the retrieval systems, the model should not assign the same weight to the retrieved labels and the label obtained by the well-trained model in computing the final prediction. Therefore, adopting a self-attention to model the relevance between the target graph and the retrieved graphs is considered to be an effective way to make use of the retrieved results while avoid sabotaging the performance of the well-trained model.

Effectiveness of Self-attention (Q2). We next investigate the effects of noisy retrieved graphs on the overall performance of our approach. In particular, we studied the situation where graphs in the training set are retrieved at random, rather than based on their similarity to the input graph. We hypothesise that, with random retrieval, the model will assign lower self-attention weights to the retrieved graphs and a much

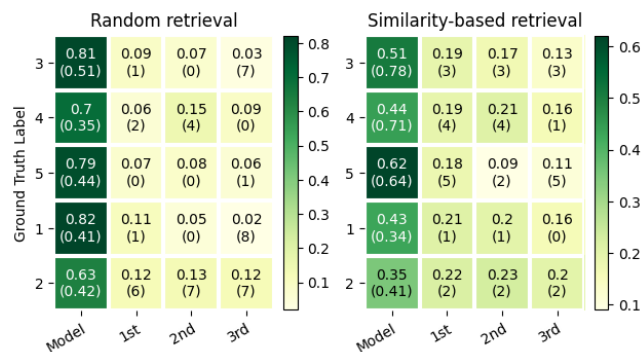


Figure 3: Results of 4 cherry-picked testing samples from CIFAR10, each of which is predicted with three similar graphs retrieved either from random retrieval approach or from similarity-based retrieval approach. In each cell, the first number represents the weight after softmax and the number in brackets is the retrieved/predicted label. For example, 0.09 (1) means that the weight for the label 1 is 0.09.

higher weight to the input graph. From Figure 3, we can observe that the model assigns higher self-attention weights to graphs retrieved based on similarity, while smaller weights are assigned to randomly retrieved irrelevant graphs. This shows that our model is noise-tolerant and will naturally assign weights to the retrieved graphs based on their usefulness.

Main Results (Q3)

Following previous studies (Hu et al. 2019, 2021), we adopted ROC-AUC as the evaluation metric for the eight molecule datasets; in turn, we used accuracy to evaluate classification performance for the MNIST and CIFAR10 datasets, and we used Mean Average Error (MAE) for regression tasks in PCQM4M and PCQM4Mv2. The obtained results are summarised in Tables 1, 4 and 5 respectively.

We can observe that the use of GRAPHRETRIEVAL significantly enhances the performance of each of the baselines, which demonstrates the effectiveness of our approach. We next discuss each of these results in further detail.

Molecule Datasets. These datasets are highly imbalanced since the label assigned to most samples is 0; The task is to predict the target molecular properties as accurately as possible, where the molecular properties are cast as binary labels, e.g, whether a molecule inhibits HIV virus replication or not. Our results are summarised in Table 1. First, we

Table 4: Classification accuracy on CIFAR10 and MNIST.

-	CIFAR10	MNIST
GCN	0.647	0.960
GIN	0.656	0.968
PNA	0.687	0.972
GRAPHRETRIEVAL-GCN	0.676(2.9% \uparrow)	0.972(1.2% \uparrow)
GRAPHRETRIEVAL-GIN	0.682(2.4% \uparrow)	0.979(1.1% \uparrow)
GRAPHRETRIEVAL-PNA	0.723(3.6%\uparrow)	0.982(1.0%\uparrow)

Table 5: MAE Performance on PCQM4M and PCQM4Mv2.

	PCQM4M	PCQM4Mv2
GCN	0.171	0.139
GIN	0.157	0.123
GRAPHRETRIEVAL-GCN	0.160(6.4% \uparrow)	0.120(1.4% \uparrow)
GRAPHRETRIEVAL-GIN	0.142(9.5%\uparrow)	0.112(8.9%\uparrow)

observe that GRAPHRETRIEVAL improves the classification performance of each of the baselines for all eight molecule datasets; furthermore, the improvements are consistent across all three baselines, which demonstrates that our approach is effective even on highly imbalanced datasets. Second, since these datasets use scaffold spitting, the substructures of the evaluation graphs are rarely reflected in the training graphs; it is therefore encouraging to observe that our approach is helpful even in such a challenging setting.

MNIST and CIFAR10. In contrast to the molecule datasets, where graphs are highly diverse and exhibit heterogeneous topologies, computer vision datasets rely on grid-structured graphs with a fixed topology (Corso et al. 2020). Our results on these datasets are shown in Table 4. We can observe that these results are consistent with those obtained for the molecule datasets, and hence our approach is also effective for computer vision problems.

PCQM4M and PCQM4Mv2. These are two large-scale datasets consisting of millions of graph instances. The task is graph regression: predicting the HOMO-LUMO energy gap in electronvolt (eV) given 2D molecular graphs. Mean Absolute Error (MAE) is used as evaluation metric. Our results on these datasets are summarised in Table 5. We found that GRAPHRETRIEVAL brings significant performance improvements on both datasets, which suggests that our approach is also beneficial for regression tasks.

Overall, our empirical results have demonstrated that GRAPHRETRIEVAL is able to bring substantial gains to GNN models. Such results are very promising because it first validates the feasibility of retrieval-enhanced approaches in the world of graph neural networks. Besides, another encouraging point is that the improvement does not come at the significant cost of increasing the model size as other models shown in some leaderboards⁴.

In what follows, we conduct additional experiments with the goal of gaining a better understanding of the different factors influencing the efficacy of our approach.

⁴<https://ogb.stanford.edu/docs/graphprop/>

Alternative Training Pipelines

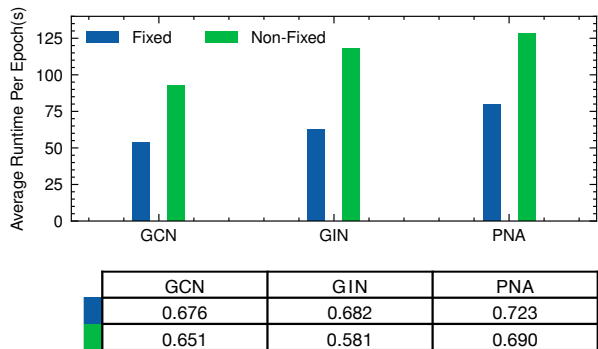


Figure 4: Results of fixed/non-fixed schemes on CIFAR10. The upper figure plots the average run time per epoch while the lower table depicts overall performance.

As already mentioned in our discussion of Algorithm 1, we train our approach in two stages: first, we train the GNN model \mathcal{M} and then we fix \mathcal{M} and train the adapter by optimising the self-attention parameters. An alternative approach would be to use the adapter training stage to further optimise the parameters of the GNN model \mathcal{M} . Obviously, the latter approach will lead to longer training times, as the number of parameters needed to be updated has increased.

To explore two different training strategies, we design a comparison experiment on the CIFAR10 dataset and the experimental results of these two approaches are summarised in Figure 4. As expected, training times are doubled if we adopt the alternative approach. However, our parameters fixed approach still achieves better performance than the alternative consistently across all three baseline GNN models. This suggests that keeping the parameters of the GNN model \mathcal{M} fixed while training the adapter simplifies the training process and makes it more stable as a result.

Case Study

To conclude this section, we cherry-pick two examples of GRAPHRETRIEVAL-PNA and PNA predicting the molecular property. In the first example, “1” is the correct label of the given input, and GRAPHRETRIEVAL-PNA gives the label=1 a much high probability compared to the PNA model. Since GRAPHRETRIEVAL-PNA manages to retrieve some similar graphs with possibly related labels, the probability solely calculated based on the input graph will be rectified. In the second example, labels of three retrieved graphs are all different from our ground-truth label, so they are considered to be noisy information. However, both of GRAPHRETRIEVAL-PNA and PNA output a similar probability for the correct label, which denotes that GRAPHRETRIEVAL-PNA is resistant to noisy information. One possible reason is that as shown in Figure 3, GRAPHRETRIEVAL will assign lower weights to those noisy labels by the self-attention mechanism. Overall, the case study shows that retrieved graphs is able to facilitate the graph property prediction and the retrieval-enhanced approach is applied to graph neural networks.

Model	Input	Predicted Probability	Retrieval
PNA	 (label=1)	$P_{label=1} = 3.34 \times 10^{-3}$	No Retrieval
GRAPHRETRIEVAL-PNA	 (label=1)	$P_{label=1} = 0.047$	( ,1) ( ,1) ( ,0)
PNA	 (label=1)	$P_{label=1} = 0.0079$	No Retrieval
GRAPHRETRIEVAL-PNA	 (label=1)	$P_{label=1} = 0.0062$	( ,0) ( ,0) ( ,0)

Table 6: Two cherry-picked examples showing how GRAPHRETRIEVAL “absorbs” useful information from retrieved graphs and “ignores” noise introduced by irrelevant graphs, respectively. In the first example, it assigns much higher probability (0.047) to the correct label, “1”, compared to PNA. In the second example when retrieved graphs are considered to be noisy information, both GRAPHRETRIEVAL-PNA and PNA assign a similar probability (0.0062 and 0.0079, respectively) to the correct label.

5 Related Work

In this section, we briefly discuss recent GNN architectures and retrieval-augmented models in Deep Learning.

Graph Neural Networks

Graph Neural Networks have become the de-facto standard for Machine Learning tasks over graph-structured data. The fundamental idea behind GNNs is that of *Message Passing*—that is, to iteratively update each node-level representation by aggregating information from its neighborhoods throughout a fixed number of layers (Kipf and Welling 2017; Gilmer et al. 2017b; Xu et al. 2018; Balcilar et al. 2021).

In molecule classification applications, Weave (Kearnes et al. 2016) explicitly learns both the atom- and bond-level representation during message passing; D-MPNN (Yang et al. 2019) emphasizes the information delivered along different directions; more recently, N-Gram Graph (Liu, Demirel, and Liang 2019) and AWARE (Demirel et al. 2021) focus on modeling the walk-level information on molecules.

The choice of the aggregation function is another key aspect of GNN design. GAT (Veličković et al. 2017) adds an attention module; GGNN (Li et al. 2015) combines information from its neighbors and its own representation with a GRU unit (Cho et al. 2014); finally, PNA (Corso et al. 2020) adopts multiple aggregation functions for combining messages.

Retrieval-augmented Models

Prior studies in different domains show that models depending only on input features and learned parameters are less powerful than models augmented by external knowledge (Lewis et al. 2020; Guu et al. 2020; Kossen et al. 2021; Wu et al. 2022; Liu, Yogatama, and Blunsom 2022).

The authors of (Wu et al. 2022) propose the use of a kNN-augmented attention layer for language modeling tasks. In (Kossen et al. 2021), the authors advocate for the use of the entire dataset (rather than using just a single datapoint) for making predictions; in particular, they show that there exist meaningful dependencies between the input and the training

dataset which are lost during training. Other related works such as REALM (Guu et al. 2020) and KSTER (Jiang et al. 2021) augment the Transformer model by retrieving relevant contexts in a non-parametric way.

In contrast to prior work, however, GRAPHRETRIEVAL focuses on the retrieval of graph-structured data. Retrieving similar graphs can be much more challenging than retrieving similar text, where pre-trained models like BERT (Devlin et al. 2018) can provide universal representations for measuring similarities. Such pre-trained models are missing for diverse graph-structured data. Furthermore, graph retrieval is also negatively affected by over-smoothing and over-squashing in existing GNNs.

6 Conclusion and Future Work

We have proposed GRAPHRETRIEVAL, a model-agnostic approach for improving the performance of GNN baselines on graph classification and regression tasks. Our main contribution is a method for exploiting the retrieval of similar graphs in the training set for making predictions, and a learnable adapter module based on self-attention for determining the influence of each retrieved graph on the final prediction. Our empirical results clearly show that GRAPHRETRIEVAL consistently improves the performance of existing GNN architectures on a very diverse range of benchmarks. We believe that our results open the door for the further development of sophisticated methods for explicitly exploiting the training data when making predictions on graphs.

Our research opens a number of interesting avenues for future work. First, it would be interesting to extend our approach to tackle node-level classification tasks. Furthermore, our approach is rather general and flexible, and we believe that it can be applied to advanced methods based on 3D geometric modeling (Schütt et al. 2017; Satorras, Hoogeboom, and Welling 2021; Liu et al. 2022; Schütt, Unke, and Gastegger 2021) as well as to a broad range of additional tasks (Gilmer et al. 2017b; Townshend et al. 2021).

References

- Balcilar, M.; Héroux, P.; Gauzere, B.; Vasseur, P.; Adam, S.; and Honeine, P. 2021. Breaking the limits of message passing graph neural networks. In *ICML*.
- Cho, K.; Van Merriënboer, B.; Bahdanau, D.; and Bengio, Y. 2014. On the properties of neural machine translation: Encoder-decoder approaches. In *CoRR*.
- Corso, G.; Cavalleri, L.; Beaini, D.; Lio, P.; and Velivckovic, P. 2020. Principal Neighbourhood Aggregation for Graph Nets. In *NeurIPS*.
- Demirel, M. F.; Liu, S.; Garg, S.; and Liang, Y. 2021. An Analysis of Attentive Walk-Aggregating Graph Neural Networks. In *CoRR*.
- Devlin, J.; Chang, M.-W.; Lee, K.; and Toutanova, K. 2018. Bert: Pre-training of deep bidirectional transformers for language understanding. *CoRR*.
- Gilmer, J.; Schoenholz, S. S.; Riley, P. F.; Vinyals, O.; and Dahl, G. E. 2017a. Neural Message Passing for Quantum Chemistry. In *ICML*.
- Gilmer, J.; Schoenholz, S. S.; Riley, P. F.; Vinyals, O.; and Dahl, G. E. 2017b. Neural message passing for quantum chemistry. In *ICML*.
- Guu, K.; Lee, K.; Tung, Z.; Pasupat, P.; and Chang, M. 2020. Retrieval augmented language model pre-training. In *ICML*.
- Hu, W.; Fey, M.; Zitnik, M.; Dong, Y.; Ren, H.; Liu, B.; Catasta, M.; and Leskovec, J. 2021. Open graph benchmark: Datasets for machine learning on graphs. In *NeurIPS*.
- Hu, W.; Liu, B.; Gomes, J.; Zitnik, M.; Liang, P.; Pande, V.; and Leskovec, J. 2019. Strategies for pre-training graph neural networks. In *ICLR*.
- Ioffe, S.; and Szegedy, C. 2015. Batch normalization: Accelerating deep network training by reducing internal covariate shift. In *ICML*.
- Jiang, Q.; Wang, M.; Cao, J.; Cheng, S.; Huang, S.; and Li, L. 2021. Learning Kernel-Smoothed Machine Translation with Retrieved Examples.
- Johnson, J.; Douze, M.; and Jegou, H. 2019. Billion-scale similarity search with gpus. *IEEE Transactions on Big Data*.
- Kearnes, S.; McCloskey, K.; Berndl, M.; Pande, V.; and Riley, P. 2016. Molecular graph convolutions: moving beyond fingerprints. In *Journal of computer-aided molecular design*, volume 30, 595–608.
- Kingma, D. P.; and Ba, J. 2015. Adam: A Method for Stochastic Optimization. In *ICLR*.
- Kipf, T. N.; and Welling, M. 2017. Semi-supervised classification with graph convolutional networks. In *ICLR*.
- Kossen, J.; Band, N.; Lyle, C.; Gomez, A. N.; Rainforth, T.; and Gal, Y. 2021. Self-attention between datapoints: Going beyond individual input-output pairs in deep learning. In *NeurIPS*.
- LeCun, Y.; Bottou, L.; Bengio, Y.; and Haffner, P. 1998. Gradient-based learning applied to document recognition. *Proceedings of the IEEE*, 86(11): 2278–2324.
- Lewis, M.; Ghazvininejad, M.; Ghosh, G.; Aghajanyan, A.; Wang, S.; and Zettlemoyer, L. 2020. Pre-training via paraphrasing. In *NeurIPS*.
- Li, Y.; Tarlow, D.; Brockschmidt, M.; and Zemel, R. 2015. Gated graph sequence neural networks. In *CoRR*.
- Liu, Q.; Allamanis, M.; Brockschmidt, M.; and Gaunt, A. L. 2018. Constrained Graph Variational Autoencoders for Molecule Design. In *NeurIPS*.
- Liu, Q.; Yogatama, D.; and Blunsom, P. 2022. Relational Memory Augmented Language Models. In *CoRR*.
- Liu, S.; Demirel, M. F.; and Liang, Y. 2019. N-gram graph: Simple unsupervised representation for graphs, with applications to molecules. In *NeurIPS*.
- Liu, Y.; Wang, L.; Liu, M.; Zhang, X.; Oztekin, B.; and Ji, S. 2022. Spherical message passing for 3d graph networks. In *ICLR*.
- Nakata, M.; and Shimazaki, T. 2017. PubChemQC project: a large-scale first-principles electronic structure database for data-driven chemistry. In *Journal of chemical information and modeling*.
- Ramsundar, B.; Eastman, P.; Walters, P.; and Pande, V. 2019. *Deep learning for the life sciences: applying deep learning to genomics, microscopy, drug discovery, and more*. O’Reilly Media.
- Satorras, V. G.; Hoogeboom, E.; and Welling, M. 2021. E (n) equivariant graph neural networks. In *ICML*.
- Schlichtkrull, M. S.; Kipf, T. N.; Bloem, P.; van den Berg, R.; Titov, I.; and Welling, M. 2017. Modeling Relational Data with Graph Convolutional Networks. In *CoRR*.
- Schütt, K.; Kindermans, P.-J.; Sauceda Felix, H. E.; Chmiela, S.; Tkatchenko, A.; and Müller, K.-R. 2017. SchNet: A continuous-filter convolutional neural network for modeling quantum interactions. In *NeurIPS*.
- Schütt, K.; Unke, O.; and Gastegger, M. 2021. Equivariant message passing for the prediction of tensorial properties and molecular spectra. In *ICML*.
- Toneva, M.; Sordani, A.; des Combes, R. T.; Trischler, A.; Bengio, Y.; and Gordon, G. J. 2019. An Empirical Study of Example Forgetting during Deep Neural Network Learning. In *NeurIPS*.
- Townshend, R. J.; Vögele, M.; Suriana, P.; Derry, A.; Powers, A.; Laloudakis, Y.; Balachandar, S.; Jing, B.; Anderson, B.; Eismann, S.; et al. 2021. Atom3d: Tasks on molecules in three dimensions. In *NeurIPS*.
- Vaswani, A.; Shazeer, N.; Parmar, N.; Uszkoreit, J.; Jones, L.; Gomez, A. N.; Kaiser, Ł.; and Polosukhin, I. 2017. Attention is all you need. In *NeurIPS*.
- Veličković, P.; Cucurull, G.; Casanova, A.; Romero, A.; Lio, P.; and Bengio, Y. 2017. Graph attention networks. In *CoRR*.
- Wu, Y.; Rabe, M. N.; Hutchins, D.; and Szegedy, C. 2022. Memorizing Transformers. In *ICLR*.
- Xu, K.; Hu, W.; Leskovec, J.; and Jegelka, S. 2018. How Powerful are Graph Neural Networks? In *ICLR*.

Yang, K.; Swanson, K.; Jin, W.; Coley, C.; Eiden, P.; Gao, H.; Guzman-Perez, A.; Hopper, T.; Kelley, B.; Mathea, M.; et al. 2019. Analyzing learned molecular representations for property prediction. In *Journal of chemical information and modeling*.

Ying, R.; He, R.; Chen, K.; Eksombatchai, P.; Hamilton, W. L.; and Leskovec, J. 2018. Graph Convolutional Neural Networks for Web-Scale Recommender Systems. In *KDD*.